PHYSICAL REVIEW B VOLUME 41, NUMBER 18 15 JUNE 1990-II

X-ray-diffraction studies of hydration transitions in Na vermiculite

N. Wada
Department of Physics, Colorado School of Mines, Golden, Colorado 80401-1887

D. R. Hines
Schlumberger-Doll Research, Old Quarry Road, Ridgefield, Connecticut 06877-4108

S. P. Ahrenkiel
Department of Physics, Colorado School of Mines, Golden, Colorado 80401-1887

(Received 15 December 1989)

Hydration phase transitions in Na vermiculite, a specific example of expandable 2:1 layered silicates, were examined as a function of temperature at a constant water-vapor pressure by x-ray diffraction. The samples exhibited well-defined 0-, 1-, and 2-water-layer hydration states (WLHS's) with the basal spacings of 9.81, 11.84, and 14.89 Å, respectively. The transitions between the hydration states were found to be first order, evidenced by a two-phase coexistence and large hysteresis. Substantial elastic deformation, which involves rotations of the tetragonal bases in the host silicate layers, was observed during the transitions. It was concluded that elastic distortion in the host layers may be responsible for the hydration phase transitions. In addition, formation of a $(2a \times 2b)$ superlattice specific to the 1-WLHS was found. A new interpretation of the previous Raman data from 1-WLHS Na vermiculite is also presented.

I. INTRODUCTION

Layered silicates, commonly known as clays, have been studied for many decades. Their properties are of high relevance to various disciplines such as chemistry, geology, agriculture, biology, mineralogy, and others.[1] Unfortunately, however, there has been little experimental or theoretical work done on layered silicates with regard to solid-state physics or physical chemistry.

Fundamentally, layered silicates provide an intriguing system with which to study intercalation and quasi-two-dimensional physics. Though graphite and heavy-metal dichalcogenide intercalation compounds have been well investigated in recent years by many physicists and chemists, layered silicates have not been studied as extensively. This is unfortunate, because the intercalation processes and resulting physical properties of layered silicates are as fascinating as those found in graphite and dichalcogenide intercalation compounds. Also, we point out that high-T_c superconducting layered ceramics exhibit structural similarities to layered silicates, e.g., compare the mica structure to the Tl-Ba-Ca-Cu-O and Bi-Sr-Ca-Cu-O compounds.[2]

Layered silicates have been used to examine several interesting physical phenomena such as *superfluidity* of hydrogen molecules.[3] When hydrogen molecules are confined in a quasi-two-dimensional space, the freezing temperature may be lowered. The boson condensation temperature for hydrogen molecules in "pillared" clays[3] may become relatively higher than the crystallization temperature, and thus one may be able to observe superfluidity. Fractal phenomena have also been studied, employing quasielastic-neutron-scattering[4] and molecular-adsorption measurements[5] from layered silicates. The fractal properties apparently arise from the size distribution of the disordered polycrystalline particles. A third set of phenomena has to do with *rigidity effects* in layered compounds. Because of the host-layer deformation due to intercalates, layered silicates exhibit a non-Vegard's-law behavior when the intercalates are a mixture of two different species.[6,7] The behavior may be understood in terms of "healing lengths" by a simple but elegant elasticity theory.[8,9]

Interlamellar cations can be replaced with magnetic ions. This allows one to examine a quasi-two-dimensional magnetic system.[10,11] For instance, Ni vermiculite exhibited a paramagnetic behavior, and at low temperatures gave evidence for successive magnetic phase transitions.[12]

Intercalation of water molecules into layered silicates is one of the most interesting phenomena. In contrast to a "staging" structure in graphite intercalation compounds (GIC's), clay intercalation compounds (CIC's) exhibit a multiple-intercalate-layer structure. Instead of having *n* host layers between nearest-neighbor intercalated layers (stage-*n* compounds in GIC's), in CIC's, *n* intercalated layers can be sandwiched by two nearest-neighbor host layers (*n*-water-layer hydration state).

In GIC's the nature of the long-range interlayer interaction responsible for staging has been intensively argued.[13,14] The interaction may originate from electrostatic repulsion or elastic deformation. In CIC's, the interlayer interaction for the long-range *c*-axis stacking sequence appears to be related to host-layer elastic deformation.

Previously, there have been some x-ray structural studies on specific vermiculite samples,[15-19] but to our knowledge, no detailed studies on the *hydration transi-*

tions have been conducted. In this paper we present x-ray-diffraction results obtained from Na vermiculite as a function of temperature at a fixed vapor pressure. Hydration phase transitions and accompanying out-of-plane and in-plane structural changes of Na vermiculite will be discussed.

In Sec. II we describe some of the basic structural and physical properties of layered silicates along with more specific properties of vermiculite. In Sec. III we describe sample preparation and experimental methods. The experimental results and discussions are presented in Sec. IV. Conclusions will be given in Sec. V.

II. STRUCTURE AND PHYSICAL PROPERTIES

Layered silicates are made of two basic sheets; one is a Si tetrahedral sheet, and the other is an Al or Mg octahedral sheet. Depending on how these basic sheets are stacked along the *c* axis, one can classify layered silicates into three categories: 1:1, 2:1 and 2:1:1 layered silicates. It is a common occurrence that some cations in the tetrahedral or octahedral sites are replaced with other cations (e.g., some Si^{4+} atoms in the tetrahedral sites are replaced with Al^{3+} atoms). Ordinarily, silicate host layers are negatively charged.

In order to compensate for the charge imbalance, cations are placed between the layers. When the host layers are severely charge deficient, the Coulombic interlayer interaction is strong. Interlamellar cations may not become hydrated (not expandable), and intercalation cannot be performed easily (no cation exchange). Micas present a good example. However, when the charge deficiency is moderate, the interlayer interaction is relatively weak. Interlamellar cations can be hydrated (expandable) and can be cation-exchanged.

Vermiculite is an expandable 2:1 layered silicate.[1] The host layer of "ideal" vermiculite consists of one Mg octahedral sheet and two Si tetrahedral sheets. One out of four Si sites in the tetrahedral sheet is replaced with an Al atom. The net charge deficiency is balanced with interlamellar cations. When the interlamellar cations are Na, for example, one can observe a zero-water-layer hydration state (0-WLHS), 1-WLHS, or 2-WLHS, of which the *c*-axis repeat distances are 9.81, 11.84, and 14.89 Å, respectively. Interlamellar cations in vermiculite can be exchanged by immersing layered silicate crystals in salt solutions. Various cation intercalated vermiculites can be prepared by this method.

The hydration state in vermiculite is determined by temperature and water-vapor pressure. Previously, hydration transitions in vermiculite have been investigated by thermogravimetric, calorimetric, and x-ray-diffraction methods.[20-22] The phase boundaries between different hydration states can be expressed with the Clausius-Clapeyron equation,

$$\frac{\partial \ln P}{\partial(1/T)} = -\frac{\Delta H_i}{R}, \quad i=1 \text{ or } 2 \tag{1}$$

where ΔH_1 and ΔH_2 are the changes of enthalpy in the transitions from a 0- to a 1-WLHS, and from a 1- to a 2-WLHS, respectively. R is the gas constant. The changes of enthalpy involved in the hydration transitions (~ 12 kcal/mol) are larger than that of bulk water (9.7 kcal/mol). This results from the interactions among the interlamellar cations, intercalated water molecules, and

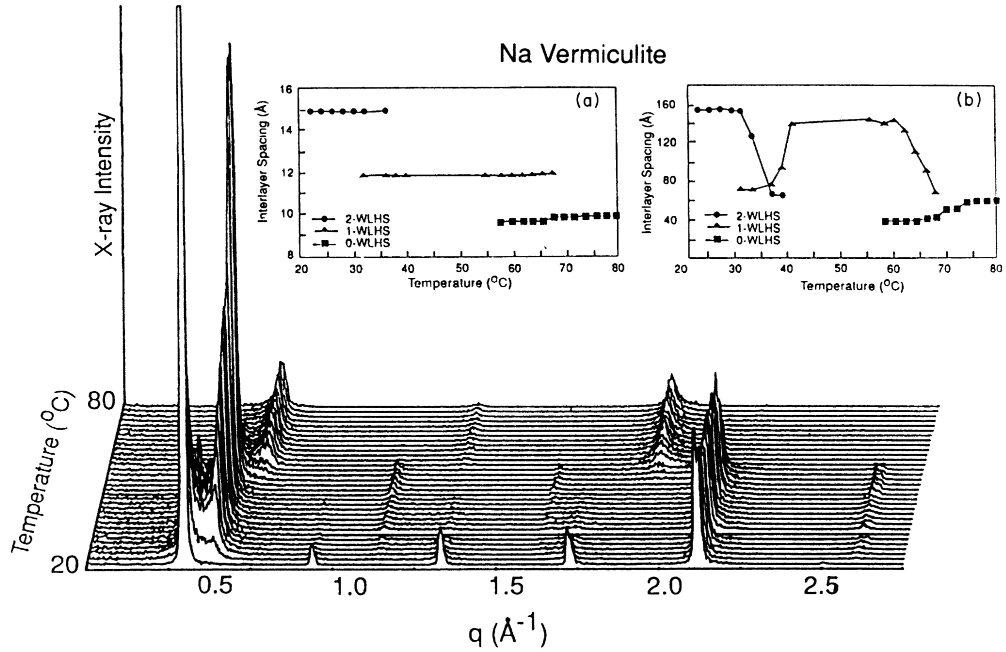

FIG. 1. (00*l*) x-ray diffraction patterns from Na vermiculite as a function of temperture at a fixed water-vapor pressure of 19.8 Torr. Inset (a) shows the basal spacing vs temperature, whereas inset (b) shows the out-of-plane correlation length vs temperature (see text).

host silicate layer.[20] In addition to the cation-water dipole interaction, the hydration of interlamellar cations involves electrostatic interactions, hydrogen bonding, van der Waals interaction, and host-lattice distortions (as will be discussed below).

III. EXPERIMENT

Our single-crystal samples originated from Llano, Texas. The chemical composition varies in the literature, but is approximately[19]

$$(\mathrm{Si}_{5.72}\mathrm{Al}_{2.28})(\mathrm{Mg}_{5.88}\mathrm{Al}_{0.10}\mathrm{Fe}_{0.03}\mathrm{Ti}_{0.02})\mathrm{O}_{20}(\mathrm{OH})_4\mathrm{Mg}_{0.93}\cdot m(\mathrm{H_2O}) ,$$

where the number of water molecules, m, varies depending on the hydration state. Llano vermiculite was chosen because of the low-iron content, good crystallinity, and uniformity of the sample quality. The samples had been cation-exchanged in NaCl solutions for more than 6 months. The completion of cation exchange was confirmed by $(00l)$ x-ray-diffraction patterns. The out-of-plane mosaic spread of the crystals was ~4°, while the in-plane mosaic spread was less than 1°. These samples are typically $10\times10\times3$ mm^3 in size.

Our x-ray-diffraction system consisted of an x-ray generator, conventional tube support (two outputs), Buerger precession camera, Huber 4-circle diffractometer with a bent-crystal graphite monochromator, and a scintillation x-ray detector. The 4-circle diffractometer was operated by a Hewlett-Packard HP-9836 computer. The software developed allowed us to conduct (hkl) scans. Mo $K\alpha_1$ ($\lambda=0.709\,30$ Å) and $K\alpha_2$ ($\lambda=0.713\,59$ Å) lines were used. The resolution of the diffractometer is limited by the bent graphite monochromator to be $\Delta k \approx 0.008$ Å^{-1} [where Δk is the full width at half maximum (FWHM)], with a Mo $K\alpha$ x-ray beam. X-ray-diffraction data were analyzed by a nonlinear least-squares-fit method.

A single-crystal sample of Na vermiculite (cut to a size of $1\times3\times0.1$ mm^3) was mounted on a goniometer, and two heaters with a platinum–versus–platinum–10% rhodium thermocouple were put close to the sample. An open-ended Kapton cover was placed over the whole sample unit. A constant flow of $\mathrm{N_2}$ gas which had gone through a water bath maintained at a constant temperature ($T=22.0\pm1.0$ °C) was guided to the sample area. Thus, the vapor pressure at the sample was at ~19.8 Torr. The sample temperature was maintained within 1 °C. At each temperature setting, the x-ray measurements were conducted after waiting for 6–12 h to make sure that the sample had reached a stable state.

IV. RESULTS AND DISCUSSIONS

X-ray-diffraction patterns obtained from Na vermiculite are shown in Fig. 1 as a function of *increasing* temperature at a fixed water-vapor pressure of 19.8 Torr.

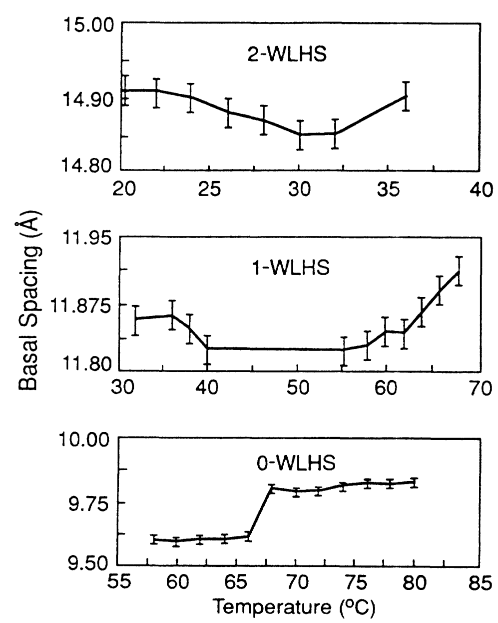

FIG. 2. d spacing vs temperature from Na vermiculite. The $(00l)$ x-ray diffraction experiments were done with *increasing* the sample temperature.

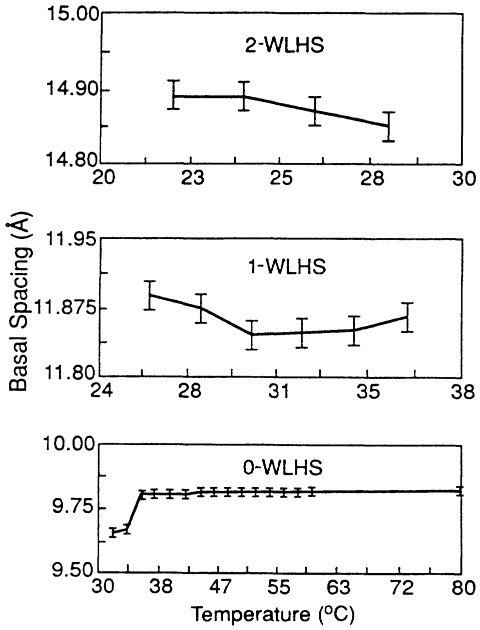

FIG. 3. d spacing vs temperature from Na vermiculite. The $(00l)$ diffraction experiments were done with *decreasing* the sample temperature.

When the Na vermiculite sample was at room temperature, it exhibited a pure 2-WLHS. The (00l) diffraction pattern yielded a d spacing of 14.89 Å and an out-of-plane correlation length of 160 Å, where the correlation length ξ is defined as $\xi = 2/\Delta q$. Δq is the FWHM of a Bragg peak.

As the sample temperature was raised to ~32 °C, there appeared a new set of Bragg peaks which corresponded to the 1-WLHS. These 1-WLHS Bragg x-ray intensities increased at the expense of the 2-WLHS peaks with increasing temperature. At 36 °C, the set of Bragg peaks from the 2-WLHS disappeared, and the sample became a pure 1-WLHS with a d spacing of 11.84±0.01 Å. The out-of-plane correlation length ξ in the pure 1-WLHS is ~140 Å, which is a little shorter than that in the 2-WLHS. We note, however, that the number of layers which correspond to those correlation lengths (ξ/d) are similar: 10.7 layers and 11.8 layers for the pure 2-WLHS and 1-WLHS, respectively. As can be seen from Inset (b) in Fig. 1, the correlation lengths for the 2- and 1-WLHS in the coexistence region are much shorter than those in the pure hydration states.

As the temperature was raised further, a set of Bragg peaks from a 0-WLHS phase started appearing at 57 °C. As before, the Bragg intensities from the 0-WLHS grew at the expense of those from the 1-WLHS. The out-of-plane correlation lengths for both the 0- and 1-WLHS were shorter in the coexistence region than in the pure-hydration-state regions. Above 68 °C, the sample became pure 0-WLHS. Unlike the other pure hydration states, the out-of-plane correlation length for the pure 0-WLHS was still relatively short ($\xi \approx 60$ Å). The x-ray patterns from the 0-WLHS Na vermiculite, which showed somewhat asymmetric peaks and nonconstant linewidths, indicated Hendricks-Teller disorder[23] in the c-axis stacking sequence. Possible causes for this disorder are (1) incomplete dehydration (intercalated water molecules could be trapped as dehydration may first occur at the edges, causing the host silicate layers to sag), and (2) in-plane disorder, where Na atoms may sit either on the pseudohexagonal cavities or on the triangular bases, resulting in slightly different interlayer distances.

Figure 2 shows plots of d spacing versus temperature from Na vermiculite, which are the same data used for inset (A) in Fig. 1, but are plotted enlarged. As can be seen from these plots, the d spacings in the three different hydration states are not constant. The d spacing in the 2-WLHS showed a slight decrease with increasing temperature, but toward the end of its existence, the 2-WLHS d spacing *increased*. The d spacing in the 1-WLHS also exhibited a similar trend. As discussed below, these c-axis lattice expansions with increasing temperature may be attributed to a structural change or lattice distortion in the host silicate layers. Na vermiculite in the 0-WLHS showed a sudden d-spacing increase at 64 °C.

The x-ray diffraction measurements were also conducted by lowering the sample temperature, otherwise with the same condition. Figure 3 shows the d spacings for

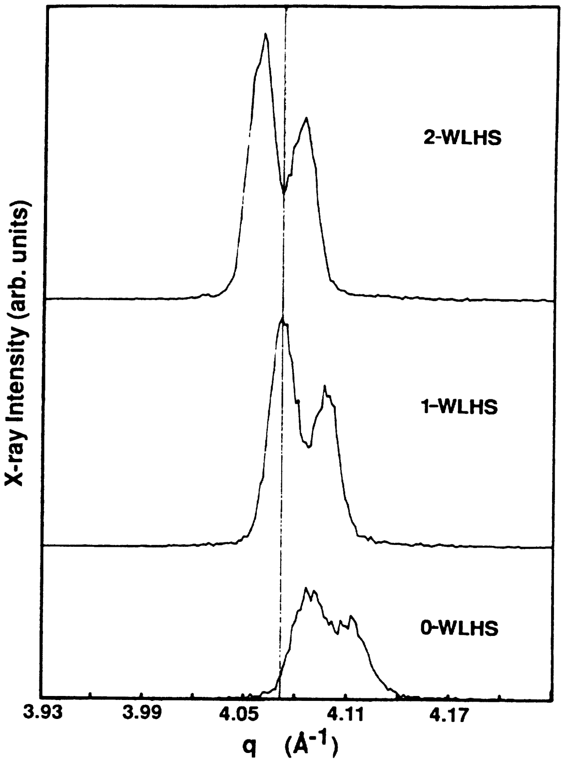

FIG. 4. (060) Bragg-peak profiles from Na vermiculite in 0-, 1-, and 2-WLHS's. The spreading of the peak originates from the Mo $K\alpha_1$ and $K\alpha_2$ lines. The abscissa shows q values calculated from the average wavelength $\lambda = 0.71145$ Å of the Mo $K\alpha_1$ and $K\alpha_2$ lines. The vertical line in the figure is for comparison of the peak positions.

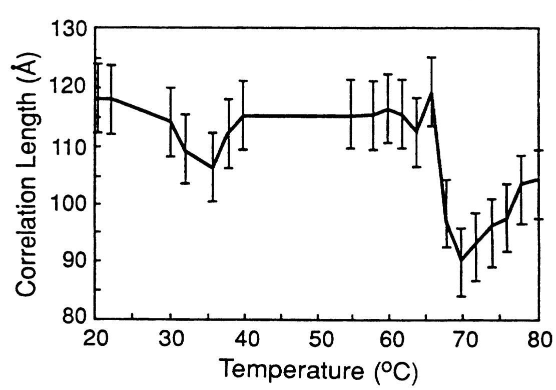

FIG. 5. Upper: lattice constant b vs temperature. Lower: in-plane correlation length vs temperature. The experiments were done increasing the sample temperature.

the three different hydration phases as a function of *decreasing* temperature. We notice first that the transition temperatures were lowered substantially, indicating a large hysteresis. The transition from the 0-WLHS to the 1-WLHS started at 36 °C, as compared to the temperature 68 °C, at which the Na vermiculite sample became a pure 0-WLHS in the increasing-temperature experiment. It is interesting to note that in both increasing- and decreasing-temperature cases the 0-WLHS d spacing showed a sudden change. The change occurred just before the 1-WLHS disappeared (increasing temperature) or appeared (decreasing temperature), which is thought to be related to a structural transition in the host silicate layers.

Further decreasing the temperature, the sample became a pure 1-WLHS at 32 °C (the pure 1-WLHS yielded $\xi \approx 140$ Å), and became a mixture of the 1- and 2-WLHS's at 28 °C. A pure 2-WLHS was obtained at 26 °C. The out-of-plane correlation length ξ after the heating cycle was found to be 150 Å, which is similar to the value obtained at the beginning. Because of the macroscopic expansion (the sample thickness changed by more than 50%), the samples sometimes became cracked. The microscopic structure of Na vermiculite, however, appeared to recover to its original shape after dehydration and hydration processes at relatively low temperatures (the maximum temperature reached was 80 °C).

The (unexpected) c-axis expansions of the d spacings in Na vermiculite discussed above may be understood if we examine in-plane structure of the host layered silicate layer. The host layer forms a rectangular lattice with typical lattice constants $a \approx 5.35$ Å and $b \approx 9.30$ Å. Since $\sqrt{3}a \approx b$, the in-plane diffraction pattern shows a pseudohexagonal symmetry.

Figure 4 shows x-ray diffraction profiles of the (060) peak from Na vermiculite in pure 2-, 1-, and 0-WLHS. The two peaks seen are from the Mo $K\alpha_1$ and $K\alpha_2$ lines (the higher-intensity peak corresponds to Mo $K\alpha_1$ and the abscissa shows q values calculated from an average wavelength $\lambda = 0.711\,45$ Å of the Mo $K\alpha_1$ and $K\alpha_2$ lines). Apparent shifts in the peak position indicate that the b-axis lattice constant of the host silicate layers varies depending on the hydration state.

Figure 5 depicts the b lattice constant and in-plane correlation lengths calculated from the (0k0) peaks from Na vermiculite as a function of *increasing* temperature.

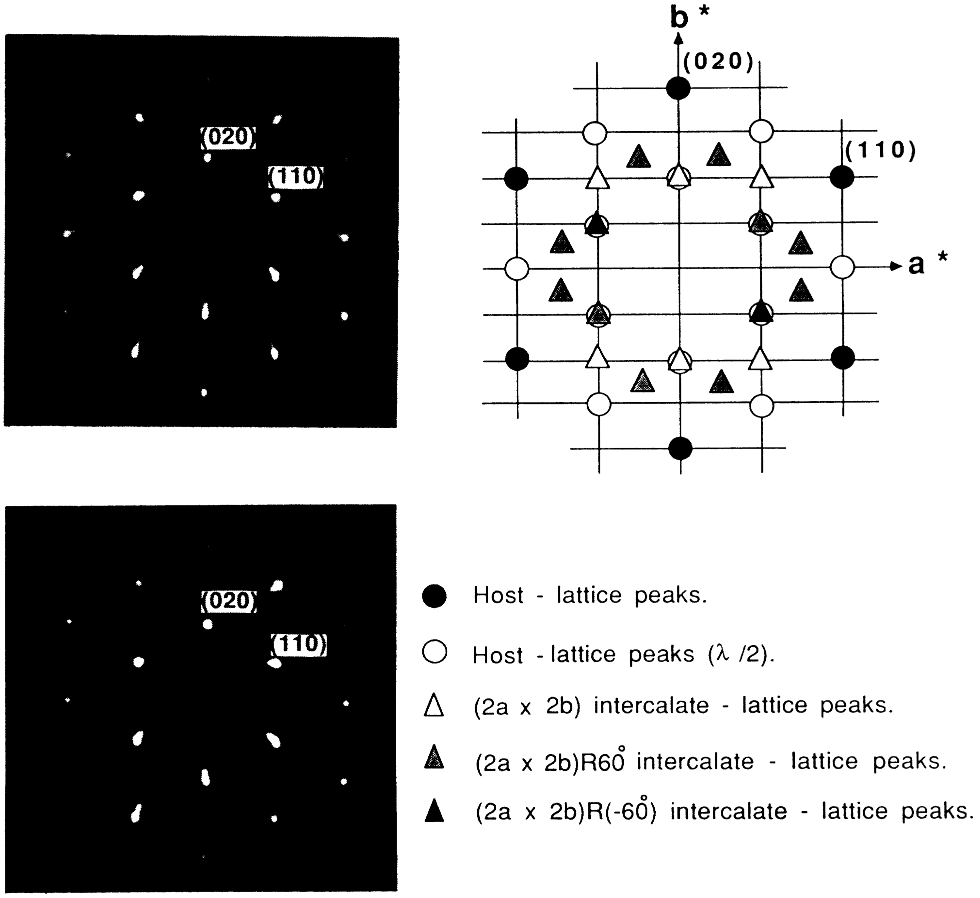

FIG. 6. Buerger x-ray precession photograph from Na vermiculite in the 1-WLHS (upper photo). An x-ray photograph from an Na vermiculite sample in the 2-WLHS is shown for comparison (lower photo). The schematic diagram shows diffraction spots from the host ($a \times b$) lattice, and the ($2a \times 2b$), ($2a \times 2b$)R60°, and ($2a \times 2b$)R(−60°) intercalate lattices. Because the films were overexposed, faint spots which correspond to $\lambda/2$ Bragg reflections are also apparent.

When the hydration state was a pure 2-WLHS, the b lattice constant was 9.30±0.01 Å. As the sample temperature was raised, the b lattice constant decreased continuously [note that the (060) peak consisted of 2- and 1-WLHS's in the coexistent region], and became constant in the pure 1-WLHS ($b = 9.27 \pm 0.01$ Å). With a further increase in temperature, the b lattice constant again decreased further in the coexistence region of the 1- and 0-WLHS's. When the hydration state became a pure 0-WLHS, the b lattice constant was stable ($b = 9.23 \pm 0.01$ Å).

It is well known that because of the misfit between octahedral and tetrahedral sheets there is a rotation of adjacent tetrahedra in opposite directions in the (001) plane. The amount of the rotation necessary to relieve the misfit is given by[24]

$$\cos\alpha = b_{\mathrm{obs}} / b_{\mathrm{ideal}} ,$$

where α is the rotation angle, b_{obs} is the observed b lattice constant, and b_{ideal} is defined as the calculated value of b for an unconstrained tetrahedral sheet. Note that the rotation does not change the lattice constant a. Thus, the contraction of the lattice constant b upon dehydration indicates more rotation of the tetrahedra.[6] Consequently, the thickness of the host layer should increase. The increase in d spacing with dehydration in Na vermiculite discussed above reflected this fact.

Figure 6 shows a Buerger x-ray precession picture from Na vermiculite in the 1-WLHS. As seen in the picture, in addition to the original host-lattice Bragg diffraction spots, there are extra spots which originate from the $(2a \times 2b)$ and $(2a \times 2b)R\,60°$ superlattices (as mentioned above, the crystal has a pseudohexagonal symmetry). X-ray pictures from the same Na vermiculite sample but in the other hydration states did not exhibit any noticeable superlattice peaks (for comparison, an x-ray picture from the sample in a 2-WLHS is also shown in Fig. 6). This implies that the interlamellar Na cations (and surrounding intercalated water molecules) for Na vermiculite in the 1-WLHS form a $(2a \times 2b)$ superlattice, but do not do so in the 0- or 2-WLHS. In the 1-WLHS the Na cations might form a pair, one cation on the tetragonal base and the other in the cavity. In the 2-WLHS the mobility of the intercalated Na ions was found to be much larger than those of 1- and 0-WLHS.[25] The Na ions may be moving around irrespective of the host-lattice layer in the 2-WLHS.

Previously, Raman spectra from Na vermiculite have been recorded as a function of hydration state.[12] Figure 7 shows the spectra. It was not understood then (1) why the A'' torsional Raman peak[6] at 105 cm^{-1} in the 1-WLHS had a narrower peak width than those corresponding peak widths in 0- and 2-WLHS's, and (2) why a new extra peak at 137 cm^{-1} appeared in the 1-WLHS.

It is now understood that the narrowing of the A'' peak at 105 cm^{-1} for Na vermiculite in the 1-WLHS may be caused by the ordering of the intercalates. The broader A'' peaks in 0- and 2-WLHS's imply that the intercalates may be disordered between the host silicate layers.

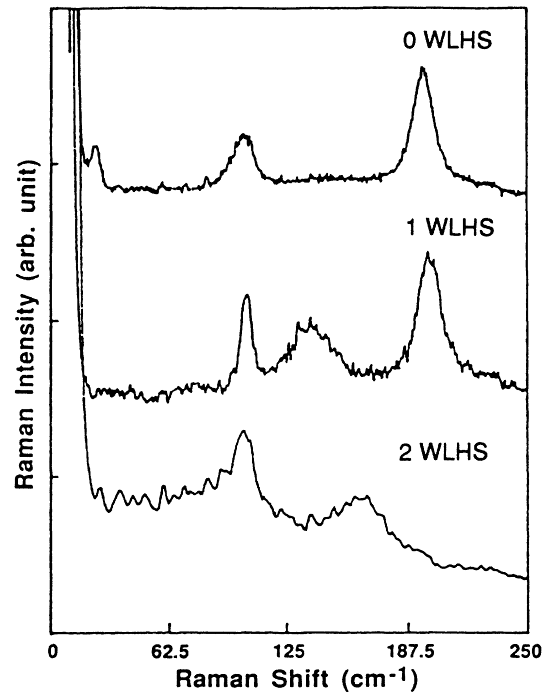

FIG. 7. Raman spectra taken from Na vermiculite in the 0-, 1- and 2-WLHS. A mode-locked 5145-Å Ar$^+$-laser beam was used in the pseudo-Brewster-angle geometry. The figure is from Ref. 12.

Also, we state that the extra peak at 137 cm^{-1} in the Raman spectrum from Na vermiculite in the 1-WLHS may be a consequence of the formation of a $(2a \times 2b)$ superlattice. Because of the doubling of the unit cell, some zone-boundary phonons could become zone-center Raman-active modes (zone folding). In fact, from the inelastic-neutron-scattering experiments of Wada *et al.*,[26] the energy of the zone-boundary in-plane LA phonon in Mg vermiculite in a 2-WLHS may be extrapolated to be 17 meV or 136 cm^{-1}. We expect that the in-plane LA mode would not be too sensitive to the interlamellar cations. The 137-cm^{-1} Raman peak from Na vermiculite in the 1-WLHS, therefore, may be assigned to be a zone-folded optical phonon from the in-plane LA branch.

V. CONCLUSIONS

It is concluded from the x-ray-diffraction experiments described above that the hydration transitions are (weakly) first order, evidenced by the coexistence of two phases and relatively large hysteresis. In the coexistence regions, from the widths of the Bragg peaks, each domain size was found to become relatively small. The correlation length of the 0-WLHS was found to be about half of that in 2- and 1-WLHS's. Possibilities such as water-molecule trapping and in-plane interlamellar disorder as reasons for the shorter 0-WLHS correlation length were suggested. The hydration transitions involve two-dimensional diffusion of water molecules between silicate layers. The large hysteresis implies that there is a substantial energy barrier for expanding the host layers upon intercalation.

It was also found that the host silicate layers experience substantial structural change during the hydration and dehydration processes (no absolute layer rigidity). The transitions in Na vermiculite involved a substantial host-lattice distortion or rotation of the tetragonal bases in the host silicate layers. This leads us to conclude that the long-range interlayer interaction responsible for the hydration transitions may be attributed to the elastic deformation of the host lattice. The detailed mechanism, however, is not understood yet. The elastic deformation should be related to the hydrogen bonding between the intercalated water molecules, the surface oxygen atoms, and the positions of the interlamellar cations.

The origin of the $(2a \times 2b)$ superlattice specific to the 1-WLHS is also not clear at this time. More work is needed to determine the *in-plane* structure of the 1-WLHS, as well as those of the 0- and 2-WLHS's, which may contribute to an understanding of the mechanism for the hydration transitions.

ACKNOWLEDGMENT

We thank Masatsugu Suzuki for fruitful discussions. Thanks are also due to G. R. Euler for technical assistance. One of us (N. W.) is grateful to Schlumberger-Doll Research for research support. This work is supported in part by the U. S. National Science Foundation under Grant No. DMR-89-13896.

---

[1] See, for instance, R. E. Grim, *Clay Mineralogy* (McGraw-Hill, New York, 1968); *Crystal Structures of Clay Minerals and Their X-Ray Identification*, edited by G. W. Brindley and G. Brown (Mineralogical Society, London, 1980); H. van Olphen, *An Introduction to Clay Colloidal Chemistry* (Wiley, New York, 1977).

[2] A. Khurana, Phys. Today **41**(4), 21 (1988).

[3] H. Deguchi, N. Morita, Y. Moriyasu, K. Takeda, S. Yamanaka, and K. Amaya, J. Phys. Soc. Jpn. **54**, 3230 (1985).

[4] P. Wong, J. Howard, and J. Lin, Phys. Rev. Lett. **57**, 637 (1986).

[5] H. Van Damme, P. Levitz, and L. Gatineau, in *Chemical Reactions in Organic and Inorganic Constrained Systems*, edited by R. Setton (Reidel, Dordrecht, The Netherlands, 1985), p. 283.

[6] B. R. York, S. A. Solin, N. Wada, R. Raythatha, I. D. Johnson, and T. J. Pinnavaia, Solid State Commun. **54**, 475 (1985).

[7] H. Kim, W. Jin, S. Lee, P. Zhou, T. J. Pinnavaia, S. D. Mahanti, and S. A. Solin, Phys. Rev. Lett. **60**, 2168 (1988).

[8] S. Lee, H. Miyazaki, S. D. Mahanti, and S. A. Solin, Phys. Rev. Lett. **62**, 3066 (1989).

[9] M. F. Thorpe, Phys. Rev. B **39**, 10 370 (1989).

[10] J. M. D. Doey, in *Proceedings of the International Clay Conference*, edited by L. G. Schultz, H. van Olphen, and F. A. Mumpton (Clay Minerals Society, Bloomington, MN, 1987), p. 261.

[11] M. Takahashi, M. Sato, S. Ishio, K. Ohtsuki, M. Suda, and M. Ono, Jpn. J. Appl. Phys. **25**, 1348 (1986).

[12] N. Wada, M. Suzuki, D. R. Hines, K. Koga, and H. Nishihara, J. Mater. Res. **2**, 864 (1987).

[13] S. A. Safran, Phys. Rev. Lett. **44**, 937 (1980).

[14] R. Clarke, N. Wada, and S. A. Solin, Phys. Rev. Lett. **44**, 1616 (1980).

[15] C. De La Calle, A. Plancon, C. H. Pons, J. Dubernat, H. Suquet, and H. Pezerat, Clay Minerals **19**, 563 (1985).

[16] J. E. Alcover, L. Gatineau, and J. Merring, Clays Clay Minerals **21**, 131 (1973).

[17] H. Shirozu and S. W. Bailey, Am. Mineral. **51**, 1124 (1966).

[18] P. G. Slade, P. A. Stone, and E. W. Radoslovich, Clays Clay Minerals **33**, 51 (1985).

[19] P. G. Slade, C. Dean, P. K. Schultz, and P. G. Self, Clays Clay Minerals **35**, 177 (1987).

[20] M. Suzuki, N. Wada, D. R. Hines, and M. S. Whittingham, Phys. Rev. B **36**, 2844 (1987).

[21] H. van Olphen, J. Colloid Sci. **20**, 822 (1965).

[22] I. Barshad, Clay Miner. **8**, 84 (1960).

[23] S. Hendricks and E. Teller, J. Chem. Phys. **10**, 147 (1942).

[24] S. W. Bailey, *Micas*, Vol. 13 of *Reviews in Mineralogy* (Mineralogical Society of America, Washington, D.C., 1984), p. 13, and references therein.

[25] M. S. Whittingham, Solid-State Ion. **25**, 295 (1987).

[26] N. Wada and W. A. Kamitakahara (unpublished).

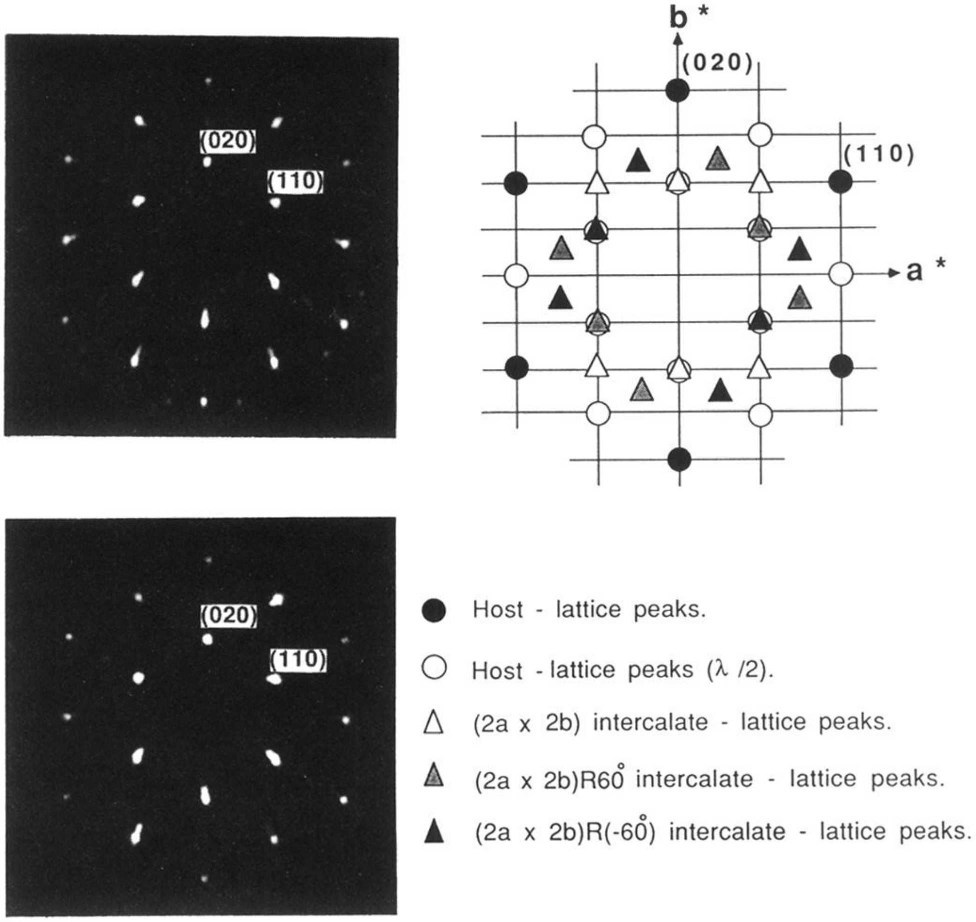

FIG. 6. Buerger x-ray precession photograph from Na vermiculite in the 1-WLHS (upper photo). An x-ray photograph from an Na vermiculite sample in the 2-WLHS is shown for comparison (lower photo). The schematic diagram shows diffraction spots from the host $(a \times b)$ lattice, and the $(2a \times 2b)$, $(2a \times 2b)R\,60°$, and $(2a \times 2b)R\,(-60°)$ intercalate lattices. Because the films were overexposed, faint spots which correspond to $\lambda/2$ Bragg reflections are also apparent.